AFRL-RX-WP-JA-2014-0185

TUNABLE STOICHIOMETRY OF BC_XN_Y THIN FILMS THROUGH MULTITARGET PULSED LASER DEPOSITION MONITORED VIA IN SITU ELLIPSOMETRY (POSTPRINT)

John G. Jones
AFRL/RXAN

FEBRUARY 2014
Interim Report

STINFO COPY

AIR FORCE RESEARCH LABORATORY
MATERIALS AND MANUFACTURING DIRECTORATE
WRIGHT-PATTERSON AIR FORCE BASE, OH 45433-7750
AIR FORCE MATERIEL COMMAND
UNITED STATES AIR FORCE

NOTICE AND SIGNATURE PAGE

_____//Signature//_____   _____//Signature//_____

JOHN G. JONES   DIANA M. CARLIN, Chief
Nanoelectronic Materials Branch   Nanoelectronic Materials Branch
Functional Materials Division   Functional Materials Division

_____//Signature//_____

TIMOTHY J. BUNNING, Chief
Functional Materials Division
Materials and Manufacturing Directorate

REPORT DOCUMENTATION PAGE

Public reporting burden for this collection of information is estimated to average 1 hour per response, including the time for reviewing instructions, searching existing data sources, gathering and maintaining the data needed, and completing and reviewing this collection of information. Send comments regarding this burden estimate or any other aspect of this collection of information, including suggestions for reducing this burden to Defense, Washington Headquarters Services, Directorate for Information Operations and Reports, 1215 Jefferson Davis Highway, Suite 1204, Arlington, VA 22202-4302. Respondents should be aware that notwithstanding any other provision of law, no person shall be subject to any penalty for failing to comply with a collection of information if it dows not display a currently valid OMB control number. PLEASE DO NOT RETURN YOUR FORM TO THE ABOVE ADDRESS.

1. REPORT DATE (DD-MM-YYYY) February 2014	2. REPORT TYPE Interim	3. DATES COVERED (From – To) 05 November 2009 – 06 January 2014

4. TITLE AND SUBTITLE
TUNABLE STOICHIOMETRY OF BC_XN_Y THIN FILMS THROUGH MULTITARGET PULSED LASER DEPOSITION MONITORED VIA IN SITU ELLIPSOMETRY (POSTPRINT)

5a. CONTRACT NUMBER
In-House

5b. GRANT NUMBER

5c. PROGRAM ELEMENT NUMBER
62102F

6. AUTHOR(S)
(see back)

5d. PROJECT NUMBER
4347

5e. TASK NUMBER

5f. WORK UNIT NUMBER
X03Z

7. PERFORMING ORGANIZATION NAME(S) AND ADDRESS(ES)
(see back)

8. PERFORMING ORGANIZATION REPORT NUMBER

9. SPONSORING / MONITORING AGENCY NAME(S) AND ADDRESS(ES)
Air Force Research Laboratory
Materials and Manufacturing Directorate
Wright Patterson Air Force Base, OH 45433-7750
Air Force Materiel Command
United States Air Force

10. SPONSOR/MONITOR'S ACRONYM(S)
AFRL/RXAN

11. SPONSOR/MONITOR'S REPORT NUMBER(S)
AFRL-RX-WP-JA-2014-0185

12. DISTRIBUTION / AVAILABILITY STATEMENT
Distribution A. Approved for public release; distribution unlimited. This report contains color.

13. SUPPLEMENTARY NOTES

14. ABSTRACT
Pulsed laser deposition is an energetic deposition technique in which thin films are deposited when a laser pulse at 248-nm wavelength strikes a target and material is subsequently deposited onto a substrate with ideally the same stoichiometry. By synchronizing a high-speed mirror system with the pulsing of the laser, and using two separate targets, thin films having tunable stoichiometry have been deposited. Depositions were performed in a high vacuum environment to obtain as much kinetic energy as possible during growth. Typically, some 150 pulses at 300 mJ/pulse were required to deposit 1 nm. Island growth must occur on a per pulse basis since over 100 pulses are required to deposit a 1 nm film thickness. Films were deposited to ~100-nm thickness, and in situ ellipsometry data were modeled to calculate thickness, n and k. X-ray photoelectron spectroscopy (XPS), Raman spectroscopy, and atomic force microscopy (AFM) were all performed on each of the films. XPS demonstrated change in film composition with change in laser pulse ratio; ellipsometry displayed thickness from the model generated as well as the optical properties from 370 to 1690 nm. AFM thickness measurements were in agreement with independently modeled ellipsometry thickness values.

15. SUBJECT TERMS
pulsed laser deposition; tunable stoichiometry; ellipsometry; multitarget

16. SECURITY CLASSIFICATION OF:

a. REPORT Unclassified	b. ABSTRACT Unclassified	c. THIS PAGE Unclassified	17. LIMITATION OF ABSTRACT SAR	18. NUMBER OF PAGES 16	19a. NAME OF RESPONSIBLE PERSON (Monitor) John G. Jones 19b. TELEPHONE NUBER (include area code) (937) 255-9106

REPORT DOCUMENTATION PAGE Cont'd

6. AUTHOR(S)

John G. Jones, Neil R. Murphy, and Rachel Jakubiak - Materials and Manufacturing Directorate, Air Force Research Laboratory, Functional Materials Division
Lirong Sun - General Dynamics Information Technology
Tyson C. Back, Matthew A. Lange, and Jessica L. Remmert
P. Terrence Murray - University of Dayton Research Institute

7. PERFORMING ORGANIZATION NAME(S) AND ADDRESS(ES)

AFRL/RXAN
Air Force Research Laboratory
Materials and Manufacturing Directorate
Wright-Patterson Air Force Base, OH 45433-7750

General Dynamics Information Technology
5100 Springfield Road
Dayton, Ohio 45431

Universal Technology Corporation
1270 North Fairfield Road
Dayton, Ohio 45532

University of Dayton Research Institute
300 College Park
Dayton, Ohio 45469

Tunable stoichiometry of BC$_x$N$_y$ thin films through multitarget pulsed laser deposition monitored via *in situ* ellipsometry

John G. Jones,[a] **Lirong Sun,**[b] **Neil R. Murphy,**[a] **Tyson C. Back,**[c] **Matthew A. Lange,**[c] **Jessica L. Remmert,**[c] **P. Terrence Murray,**[d] **and Rachel Jakubiak**[a]

[a]Air Force Research Laboratory, 3005 Hobson Way, Wright-Patterson AFB, Ohio 45433
john.jones.66@us.af.mil
[b]General Dynamics Information Technology, 5100 Springfield Road, Dayton, Ohio 45431
[c]Universal Technology Corporation, 1270 North Fairfield Road, Dayton, Ohio 45532
[d]University of Dayton Research Institute, 300 College Park, Dayton, Ohio 45469

Abstract. Pulsed laser deposition is an energetic deposition technique in which thin films are deposited when a laser pulse at 248-nm wavelength strikes a target and material is subsequently deposited onto a substrate with ideally the same stoichiometry. By synchronizing a high-speed mirror system with the pulsing of the laser, and using two separate targets, thin films having tunable stoichiometry have been deposited. Depositions were performed in a high vacuum environment to obtain as much kinetic energy as possible during growth. Typically, some 150 pulses at 300 mJ/pulse were required to deposit 1 nm. Island growth must occur on a per pulse basis since over 100 pulses are required to deposit a 1 nm film thickness. Films were deposited to ∼100-nm thickness, and *in situ* ellipsometry data were modeled to calculate thickness, *n* and *k*. X-ray photoelectron spectroscopy (XPS), Raman spectroscopy, and atomic force microscopy (AFM) were all performed on each of the films. XPS demonstrated change in film composition with change in laser pulse ratio; ellipsometry displayed thickness from the model generated as well as the optical properties from 370 to 1690 nm. AFM thickness measurements were in agreement with independently modeled ellipsometry thickness values. © *2014 Society of Photo-Optical Instrumentation Engineers (SPIE)* [DOI: 10.1117/1.JNP.8.083999]

1 Introduction

Nanotechnology applications require material feature sizes or structures between 1 and 100 nm. Thermal materials, optical materials, metamaterials, and many others are all examples of areas which would greatly benefit from films having improved properties of interest such as thermal conductivity, resistivity, refractive index, or chemical stability, as well as required nano-sized features. A current significant problem is being able to obtain material samples having precise material composition uniformity on the nanometer scale. The novelty of this paper is that by synchronizing a pulsed laser with two different pulsed laser deposition (PLD) target materials and a programmable galvanometer, the stoichiometry of a film can be tuned at the subnanometer scale resulting in thin film growth having either constant or functionally graded composition. If a particular PLD target requires approximately 130 laser pulses to generate 1-nm thickness at a substrate, then clearly on a per pulse basis island growth occurs. Island growth results from a few laser pulses on a target, and by repeatedly applying a fixed number of pulses onto each PLD target an amorphous thin film can be generated at room temperature having a desired composition that is very well mixed at the subnanometer level throughout the thin film.

Each different composition results in different material properties and is expected to be defined by the rule of mixtures. PLD is an efficient vacuum deposition technique for depositing films from a target material, with compressive stresses ultimately defining the maximum thickness for each different film of interest.[1] To illustrate this novel growth technique, BC_xN_y was chosen as a materials system with PLD targets of BN and C used as basic components. Three amorphous thin films 100 nm or less in thickness were deposited using this novel technique to illustrate the resulting tunable amorphous materials properties, as well as films of pure BN and C.

BC_xN_y thin films are of interest due to their potential to be more chemically stable and oxidation resistant at higher temperatures as compared with pure carbon based materials.[2] BN has a wide band gap, >5.0 eV for different phases such as hexagonal or cubic, making it a good insulator and when in the cubic form is not as hard as diamond, but is more chemically stable. BC_xN_y is also more chemically stable than carbon with both BC_4N nanotubes stable to decomposition in air up to 900°C, as well as hexagonal BN (h-BN) to 1000°C.[3] Oxidation resistance testing was beyond the scope of this effort, but motivated the choice of materials. For future efforts, the films will need to be deposited at high temperatures to obtain crystalline bonding, instead of strictly amorphous thin films that result from room temperature deposition. Novel photonic applications involving high temperature thermal management and index matching could be well suited to use BC_xN_y, such as optical metamaterials for high temperature application.

In situ spectroscopic ellipsometry was employed in order to characterize optical properties from 370 to 1690 nm.[4] Ellipsometric analysis measures the change in the polarization of light after subsequent reflection through a medium. By analyzing the phase difference (Δ) and magnitude (Ψ) of the refracted, elliptically polarized light, ellipsometry can provide information pertaining to several optical and physical properties of the film during growth.[5] Due to the different optical behaviors of various classes of materials, raw ellipsometry data must be fit using an appropriate model. Successful fitting of experimental data can lead to an accurate estimation of the material's refractive index (n), extinction coefficient (k), and thickness. The final thickness calculated from the models generated from ellipsometry data was verified with atomic force microscopy (AFM). X-ray photoelectron spectroscopy (XPS) and Raman spectroscopy were used to measure and compare the composition of the films.[6] In this paper, four different desired thin film compositions were deposited and compared: (a) 100% BN, (b) 80% BN–20% C, (c) 67% BN–33% C, and (d) 50% BN–50% C. Addition of C to the film increased the extinction coefficient and caused the film to be much more opaque.

2 Experimental Setup

As shown in Fig. 1, a Lambda Physik LPX 220 excimer laser was used to ablate material from two different 50.8 mm rotating target materials of 6.3-mm thick. The target to substrate distance was 125 mm. The laser was pulsed in a synchronous fashion at ~16 Hz by computer software which also constrained the laser beam path using a Cambridge Technology galvanometer system (two axes servo mirror system with capacitive coupled position feedback for high speed) to a uniform elliptical pattern on each target, and pulsed the required number of pulses sequentially
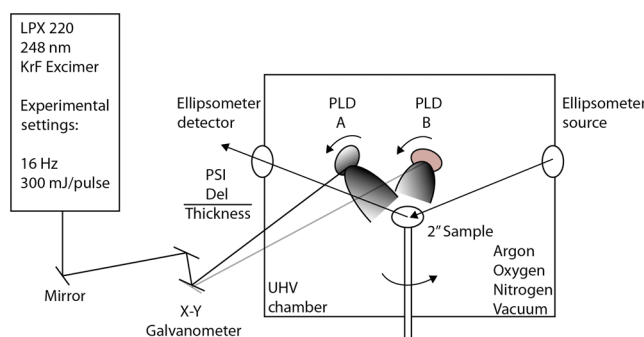

Fig. 1 Pulsed laser deposition (PLD) process utilizing multitarget galvanometer: PLD A–carbon and PLD B–BN.

on each target. For each of four depositions 13,000 pulses at 300 mJ/pulse were used with different ratios of BN to C: 100% BN–0% C, 80% BN–20% C, 67% BN–33% C, and 50% BN–50% C. These ratios were achieved by placing the following sequence of pulses of BN and then C in a repeated fashion: 100–0, 16–4, 16–8, and 8–8. Each trigger event of the excimer laser generated a 20 ns output pulse at 300 mJ of 248 nm light having $\sim$60 J/cm^2 that created a plume of ablated material which was visible for <20 μs.[7] Each laser pulse is 24 mm × 8 mm as measured at the laser, before focusing. The laser output was focused to strike the center of the target with a focused spot size of approximately 1.2 mm × 0.4 mm. The depositions were performed in high vacuum (HV) to be as energetic as possible, with initial base pressures $\sim$9.3 × 10^{-5} Pa.[8]

Ellipsometry data were collected *in situ* using a Woollam M2000, and ellipsometry modeling was performed by using a multilayer model which consisted of a substrate model for silicon, a SiO$_2$ layer for the oxidation layer that is always initially present on silicon, and a second modeled layer representative of the data collected *in situ* during the thin film deposition. After a model is generated matching each of the three modeled layers, the film thickness can be calculated.

Initial alignment verification and data collection were performed for each sample and the native silicon oxide thickness was calculated to be $\sim$2.25 nm for each wafer. A model generated parameters defined to constantly fit the data generated during deposition, and the primary parameter of interest for modeling was the real-time thickness. The thickness measured for 100% BN thin film by ellipsometry was 100 nm at completion. Samples were analyzed with a Renishaw inVia Raman microscope, Staib XPS, and Asylum Research MFP3D AFM.

3 Results and Discussion

Ellipsometry data were collected for each of four deposition conditions and used to calculate n and k at five exemplary wavelengths as well as the final film thickness. Table 1 shows the numerical n and k results at one of the five wavelengths, 632 nm, for each of the experimental conditions. The ellipsometer model used contains three layers: the first layer is an infinitely thick silicon substrate, the second layer is the native silicon oxide layer, and the third layer is a dynamic model of the grown thin film. The silicon substrate and native oxide were measured prior to deposition process and were assumed to remain unchanged. The parameters shown in Table 1 were calculated using a Tauc-Lorentz model, due to its ability to accurately characterize the optical behavior of amorphous materials, including carbon and various nitrides.[9–11] Throughout the deposition process, raw psi (Ψ) and del (Δ) data were analyzed within the J.A. Woollam CompleteEase software package using a Cauchy model because of its simplicity and small mean squared error. Numerical components of the model were continuously optimized to approximate n and k across the wavelength range of the device. The thickness of the growth layer was both calculated and displayed every 8 s.

3.1 *XPS Characterization*

XPS characterization was performed on each sample using a Staib XPS system consisting of an ion pump, x-ray source, and energy analyzer. Samples were loaded into an antechamber with a base pressure of 6.7 × 10^{-6} Pa or better. The samples were then transferred into the analysis

Table 1 Ellipsometer summary of film growth on Si wafer with $\sim$2.25 nm oxide layers.

PLD A–carbon (%)	PLD B–BN (%)	Thickness (nm)	n_{632}	k_{632}
0	100	100	2.02	0.006
20	80	91	2.04	0.056
33	67	88	2.14	0.145
50	50	85	2.36	0.304

4

chamber which had a base pressure of 4.0×10^{-8} Pa. XPS data were collected using a pass energy of 20 eV. All spectra were background corrected using a Shirley background subtraction. Component curves were fitted to each spectrum using a Levenberg−Marquardt algorithm that minimizes χ^2, Fig. 2. Each component curve consists of a convolution of Gaussian and Lorenztian functions. Photoemission intensities were corrected to account for Scofield cross sections, kinetic energy, and analyzer transmission function. XPS data were collected with a standard Mg $K\alpha$ (1253.6 eV) excitation source. The energy scale was calibrated against Au $4f_{7/2}$ and Cu $2p_{3/2}$ at the binding energies of 84.0 and 932.6 eV, respectively. The XPS resolution was determined by the FWHM of the Au $4f_{7/2}$ line, which was found to be 1.2 eV.

Table 2 shows the binding energy (E_B) for boron and carbon (B 1s and C 1s). The normalized concentration of each element is equal to the measured intensity divided by the instrument sensitivity factor for that element. The resulting percentage of the normalized concentration for each element is then the atomic percent. Table 2 shows the surface characterization measurements for the 50% C-50% BN sample. Oxygen contamination, O 1s peak, is shown as being some 28%; this is expected due to the fact that the samples have been exposed to air and were exposed to an ion beam for a brief time before sampling. The same measurement and analysis techniques were used on each of the four samples. Table 2 shows that the ratio of B 1s to C 1s is approximately slightly <1.0 and the ratio of B 1s to N 1s is just under 1.7.

Figure 2 shows plots of the binding energies for boron and carbon 1s peaks. The spectra show cross-contamination that occurred during growth, and are obvious for the first growth of 100% BN, i.e., a laser pulse of carbon would place small amounts of carbon onto the BN target, and pulse onto the BN target would contaminate the carbon target. This issue has been largely resolved with the addition of a shutter over the sample as well as a shield between the two PLD targets which provides for the ability to operate the ellipsometer even while the shutter is closed with PLD operating for the purposes of precleaning the targets, and has been shown to be required.

Figure 2 shows the composition summary of B, C, and N for each of the four films deposited and the corresponding XPS composition. The nitrogen content is lower than boron content for each sample, which can be explained by the fact that ionization and atomization of the BN target during the PLD process in vacuum results in a loss of nitrogen. Since the pressure was constant, HV, it was also expected that the same boron to nitrogen ratio will essentially be maintained
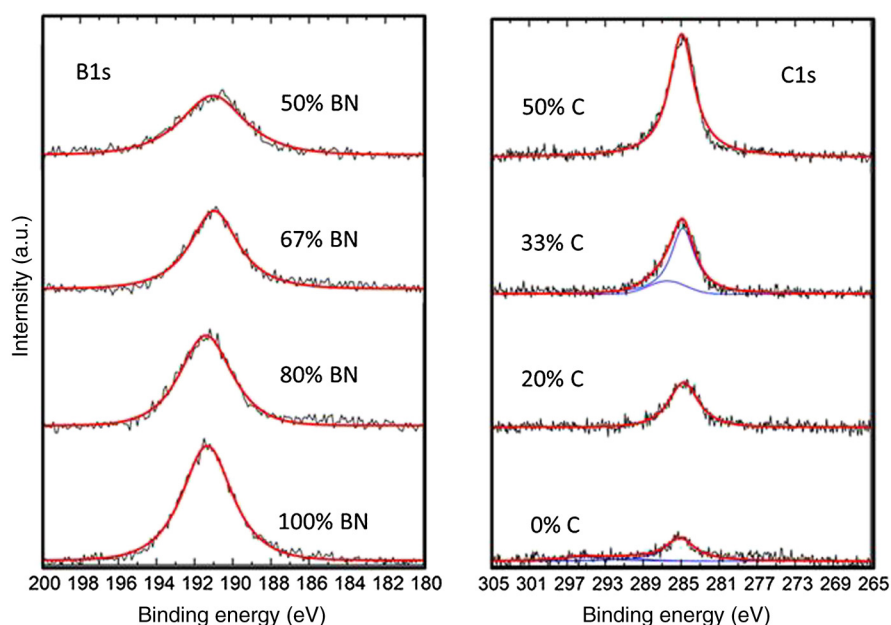

Fig. 2 X-ray photoelectron spectroscopy (XPS) showing boron opposite of carbon for desired BN: C ratio. Both sets of stacked spectra consist of raw data (black), fitted components (blue), and sum curves (red).

Table 2 X-ray photoelectron spectroscopy surface characterization of 50% carbon–50% BN sample. Measurement error is ±0.1 atomic %.

Element	E_B (eV)	Measurement intensity (a.u.)	Sensitivity factor	Normalized concentration	Quantity (atomic %)
B 1s	191.0	1146.51	1.184	968.33	26.6
C 1s	285.0	2932.08	2.73	1074.02	29.6
N 1s	398.8	2187.55	3.789	577.34	15.9
O 1s	532.9	2406.50	2.37	1015.40	27.9

regardless of BN:C ratio of growth, as shown in Fig. 3, and the B:N ratio is ~1.5 for XPS characterized samples.

The desired growth setpoints that were also characterized by XPS were BN: 100%, BN: 80%, BN: 67%, and BN:50%, but as is shown in Fig. 3, the actual boron to carbon ratios ended up being 4.33, 2.96, 1.44, and 0.901, respectively. The ratio of boron to nitrogen ended up being 1.472, 1.493, 1.480, and 1.678, respectively. This represents ratios on the order of ~B_4CN_x, ~B_3CN_x, as well as two samples with a ~BCN_x ratio near unity, i.e., one B:C sample rich in boron and the other rich in carbon.

As was previously mentioned, the four samples grown without mechanical shielding between targets and characterized by XPS show approximately a 4:1 ratio of boron to carbon for the first sample which should not have had any significant amount of carbon. This error can be from either XPS measurement technique due to air exposure, or due to contamination occurring during the deposition process. Contamination can occur by the fact that if the targets are not physically separated using mechanical shielding, then each laser pulse will have material both deposited on the substrate, but also onto the other laser target and thereby skewing the desired deposition parameters and potentially creating particulates. To test this, six additional samples were grown to approximately 1 μm in thickness with mechanical shielding added between PLD targets to prevent cross-contamination. Energy dispersive x-ray characterization was performed with a Hitachi 3000 tabletop SEM with energy-dispersive X-ray spectroscopy (EDX) attachment. As shown in Fig. 3, the results were virtually identical within the error in terms of composition. However, the first XPS sample shown with a C:B ratio of ~0.25 demonstrates the first sample was contaminated as the EDX sample shows a carbon content of zero as expected, Fig. 3.
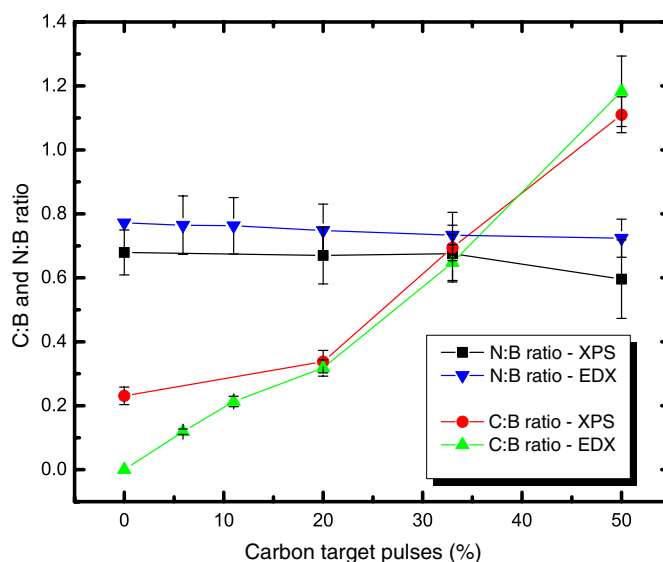
Fig. 3 XPS and EDX summary of B:N ratio (atomic %) and B:C ratio for each setpoint of carbon target pulses (%).

6

PLD results in a direct stoichiometric transfer of material from target to substrate, but in vacuum also in all directions, hence the need to have a shield between targets to prevent cross-contamination. Adding a mechanical shield prevented cross-contamination issues.

When depositing from the BN target, there is a loss of nitrogen (Fig. 3, N:B ratio below 1) due to the fact that the deposition is being performed in vacuum, which is typical for multielement targets containing nitrogen or oxygen. One of many techniques to raise the resulting thin film nitrogen content is to perform depositions at a pressure of a few Pa of nitrogen. Figure 3 demonstrates that the composition, C:B ratio, can be adjusted with precision using PLD, but optimization process with regard to BC_xN_y would need to be performed to obtain the desired nitrogen content as well. For single element targets, it is clear that subnanometer mixing can be accomplished using sequential laser pulses on each target.

3.2 *Raman Characterization*

Figure 4 shows four Raman spectra corresponding to each of the four samples and a carbon sample for the reference. A Renishaw inVia Raman microscope having a 514 nm laser excitation and 50× microscope objective was used for the measurements in a confocal mode providing a measurement depth of approximately 1 μm. The peaks shown in each of the spectra below 1000 cm^{-1} are from the Si substrate and corresponding native oxide layer of SiO_2 (∼2.25-nm thick). The carbon sample was deposited with the same conditions as the other four, but for a much shorter period of time yielding a film thickness of ∼30 nm, and as such the Si and SiO_2 peaks are much larger than those observed in the other samples.

Raman spectra of carbon are expected to have a D peak at 1360 cm^{-1} and a G peak at 1580 cm^{-1}, and boron nitride is expected to have Raman peaks at 1055 cm^{-1} for cubic BN (c-BN) and 1364 cm^{-1} for hexagonal BN (h-BN).[12] As is shown in Fig. 4, the spectra above 1000 cm^{-1} are as could be expected, essentially a D peak component, a much larger G peak component, and second harmonic of the D peak. By peak fitting the D and G components using two Gaussian functions, for pure carbon, the algorithm returns that there is dominantly graphitic carbon having a G peak centered at 1557 cm^{-1} and a much smaller D peak centered at 1401 cm^{-1}, and for the pure BN sample, there is only h-BN with a broad peak centered around 1300 cm^{-1}. The D peak and h-BN peak overlap and the peak position of their summation shifts lower in wavenumber with the increasing BN content. Since the depositions were performed
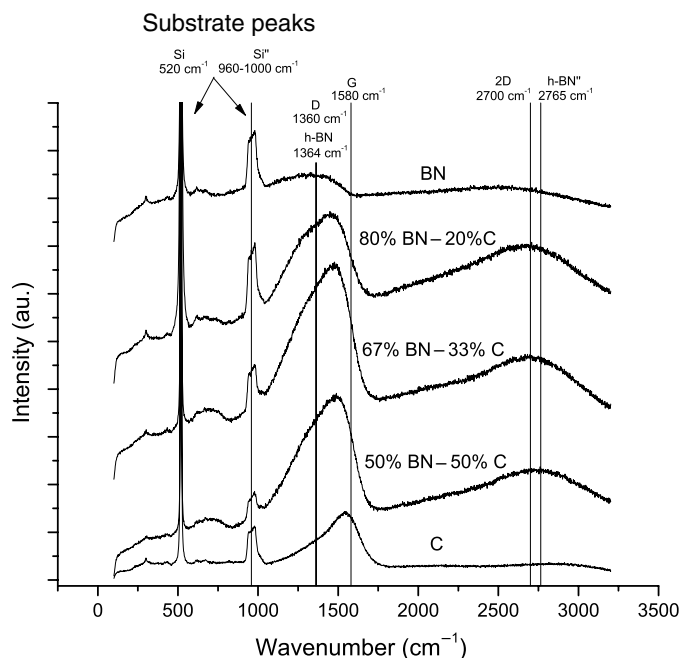

Fig. 4 Raman spectra of each of the five samples as deposited.

without a heated substrate c-BN was not expected to be formed, which is confirmed by the absence of a 1055 cm^{-1} peak. The spectra in Fig. 4 for 80% BN-20% C deposited by PLD are equivalent to the Raman spectra presented in Ref. 13 from sputtering of B_4C in 10% N_2 to obtain a film composition of 48% B, 12% C, and 40% N.[13]

Beginning with the pure carbon sample Raman spectra, increasing the amount of BN causes the G peak to be reduced relative to the h-BN peak as the boron content is increased, and hence the h-BN peak of 1364 cm^{-1} is increased in intensity. The broad peak around 2700 cm^{-1} is the second harmonic of the ~1360 cm^{-1} peak. The second harmonic of bulk h-BN (h-BN'') is represented by a broad peak at 2765 cm^{-1}, while the BN thin film second harmonic is ~2500 cm^{-1}, Fig. 4.[14]

One noticeable detail is that with each of the four films having approximately the same thickness, the pure BN film has a Raman intensity at ~1300 cm^{-1}, which is much smaller than the substrate related to peak intensity at ~970 cm^{-1}. This lack of Raman response for pure BN would imply that either the film is not nearly as thick or that BN is perhaps much more transparent to 514 nm laser excitation than carbon. The film thickness was verified with ellipsometer modeling, AFM, and a KLA Tencor profilometer, so the lack of response must be from the actual material properties such as the absorption coefficient at 514 nm.

3.3 *AFM Characterization*

An MFP3D AFM (Asylum Research) was used to measure film thickness and surface root-mean-squared (RMS) roughness for each sample composition. The data shown in Fig. 5 were acquired in ac (tapping) mode by an Olympus ac160 silicon probe with a nominal tip radius of 9 ± 2 nm. Sample thickness was measured relative to the silicon substrate (disregarding an uneven edge formed by the removal of a mask adjacent to the deposited film). A measured thickness of 103.7 nm is indicated by the cross section in Fig. 5(a) for a BN-50:C-50 scan. An image analysis function in the MFP3D (Igor Pro-based) software was used to calculate the RMS roughness of unmodified topography data according to $\sqrt{(1/n) \sum z_i^2}$, where n is the total number of z height values. Figure 5(b) shows a representative 10 μm scan of BN-80: C-20, which yielded a full image RMS value of 7.87 nm. RMS values were on the order of 7 to 11 nm for randomly sampled 10 μm areas. The horizontal lines in Fig. 5(b) were artifacts from the instrument of the tallest features in the scan line. The particulates captured in Fig. 5(b), displayed as white spots, were observed for each sample composition and could be attributed to the deposition of material onto the opposing PLD target with the ablation pulse. Each focused laser pulse was approximately 1.2 mm × 0.4 mm, with each target material having
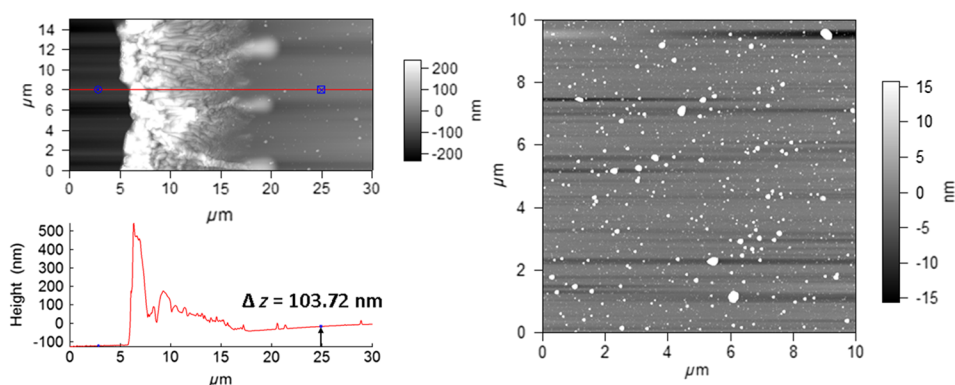

Fig. 5 Atomic force microscopy (AFM): (a) height profile across the edge of a BN-50:C-50 sample indicates approximate 100 nm film thickness relative to the silicon substrate. The uneven edge morphology was formed by the removal of a mask after deposition. (b) Representative 10 μm BN-80:C-20 surface scan yields 7.9 nm RMS roughness. RMS values were ~7 to 11 nm over randomly sampled 10 μm areas, and the surface morphology is typical for the four compositions evaluated. Particulate heights range between <10 and >100 nm; horizontal lines across the tallest features are AFM scanning artifacts.

some 45-mm diameter active area of ablation, allowing buildup of particulates from many pulses onto each opposite target before an actual deposition pulse. In this manner, some degree of particulates are expected, but could be mitigated with the addition of a shield between the laser targets.[15]

3.4 *In Situ Ellipsometer Characterization*

In situ ellipsometer data were collected for each of the four depositions, with the 50% BN–50% C and the 80% BN–20% C deposition dynamic data being shown in Fig. 6. Each deposition lasted approximately 15 min, with the deposition conditions being 300 mJ/laser pulse, and a 16 Hz pulse rate from the laser. During the deposition, the growth rate of the thin film thickness was linear as shown in Figs. 6(c) and 6(d). The value of Ψ changed significantly during growth with each associated wavelength. The effect of different composition of materials and the difference in optical property of the material was significant, with the 80% BN–20% C having the largest change in the magnitude of Ψ. The change in Ψ is most pronounced at 371.3-nm wavelength, Figs. 6(a) and 6(b).

The ellipsometer measures psi and del across the wavelength range of 370 to 1690 nm. CompleteEase software from J.A. Woollam provides for definition of optical layers, and in this case, a modeled layer for the Si wafer substrate, the SiO_2 native oxide layer, and a Cauchy model for each thin film of interest. Each optical layer is parameterized by the thickness, n and k, and an appropriate model such as Tauc-Lorentz, Sellmeier, or in the simplest form Cauchy for transparent materials. The CompleEase software iteratively fits all measurements to all of the defined model layers to determine optimal model parameters. The Cauchy model, Eqs. (1) and (2), is an approximate function of the Sellmeier model in which a series expansion is used to compute $n(\lambda)$ and $k(\lambda)$:
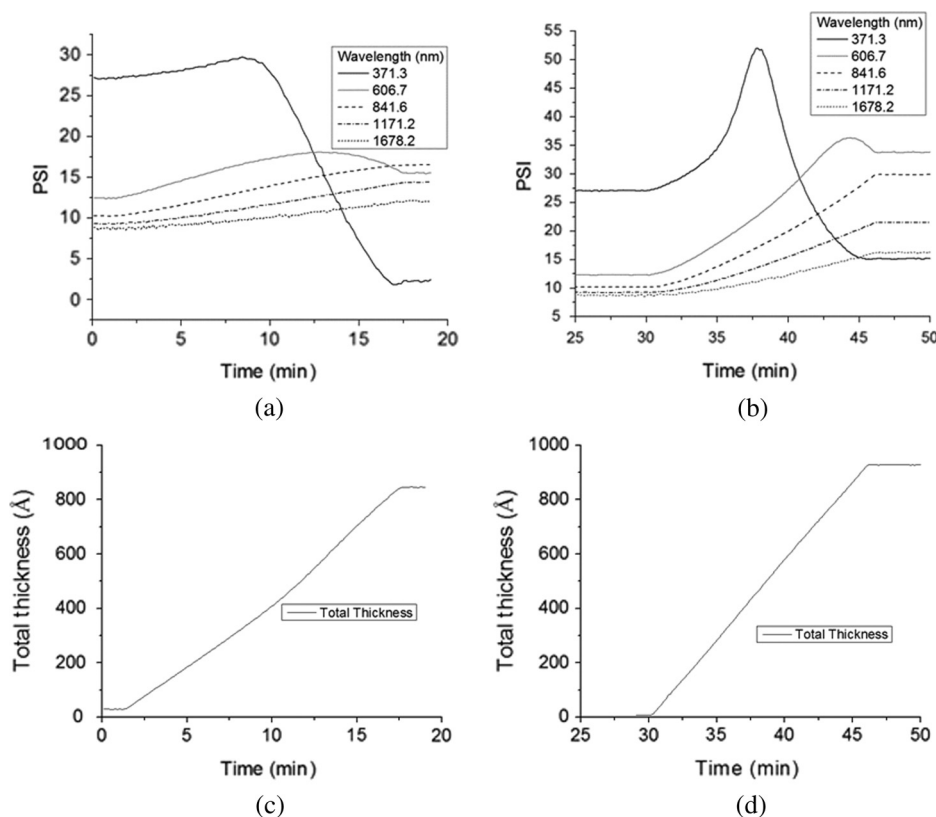

Fig. 6 Dynamic ellipsometer spectra collected during deposition: (a) BN-50:C-50 and (b) BN-80: C-20. *In situ* thickness modeled using ellipsometry (c) for BN-50:C-50 and (d) for BN-80:C-20.

$$n(\lambda) = A + \frac{B}{\lambda^2} + \frac{C}{\lambda^4}, \tag{1}$$

$$k(\lambda) = k1 \cdot e^{k2(E-E_B)} = k1 \cdot e^{k2\left[12400\left(\frac{1}{\lambda} - \frac{1}{\text{Band Edge}}\right)\right]}. \tag{2}$$

In Eq. (1), the constant A represents the approximate index of refraction and together with B and C define the index dispersion. Band edge is a parameter in nanometers that is set manually, whereas the $k1$ and $k2$ paramters determine the shape of the extinction coefficient dispersion. Once the best fit of the parameters A, B, C, $k1$, and $k2$ are obtained by CompleteEASE, where n and k and thickness are calculated.

From a Cauchy model fit of the psi and del *in situ* data of two deposition conditions, n and k were calculated at five representative wavelengths for the 50% BN–50% C and 80% BN–20% C cases, Fig. 7. The 50% BN case shows that particular film is very absorptive, especially at 514 nm where strong Raman spectra were collected, and the 80% BN case was not nearly as absorptive, Fig. 7. The extinction coefficient for pure BN, Fig. 7, was closest to zero at 514 nm as compared to the others, and was correspondingly the weakest Raman scattering thin film at 1364 cm^{-1}, Fig. 4.

Additionally, all samples n and k values are shown in Fig. 7: pure BN, 80% BN–20% C, 67% BN–33% C, 50% BN–50% C, and pure carbon. BN has the lowest value of index of refraction of the films grown at 2.0, and carbon the highest around 2.4.[15] As demonstrated in Fig. 7, changing the stoichiometry by adding amounts of carbon will cause a shift in the actual optical properties of index of refraction and absorption coefficient, which can be desired for filters, optical lenses,
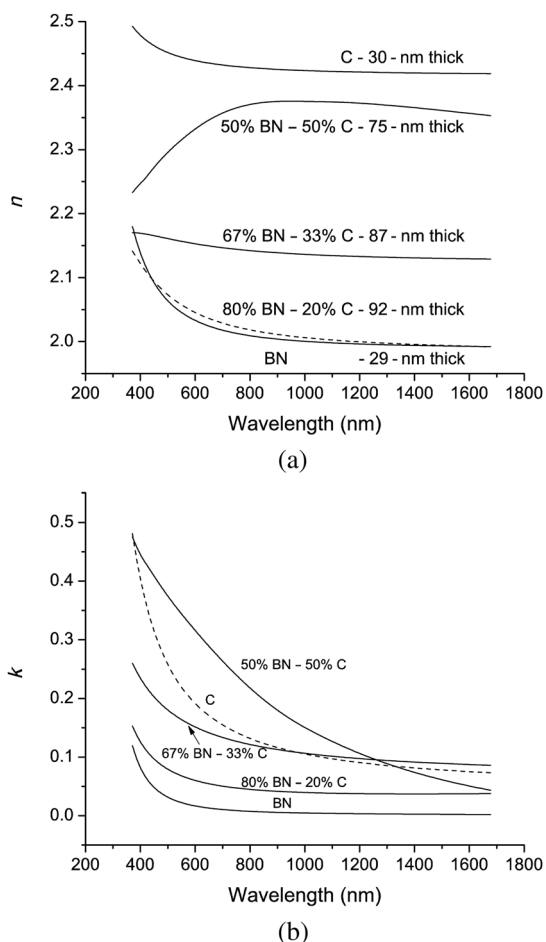

Fig. 7 n (a) and k (b) with the wavelength for pure BN and samples having tuned stoichiometry ~100 nm in thickness and C ~30-nm thick.

Table 3 Changes of n and k according to carbon concentration at 632 nm.

PLD A–carbon (%)	PLD B–BN (%)	Carbon (atomic %)	n_{632}	k_{632}
0	100	0	2.02	0.006
20	80	15	2.04	0.056
33	67	27	2.14	0.145
50	50	41	2.36	0.304

coatings, metamaterials, or other applications. Increasing carbon concentrations, Table 3, show that when compared at a specific wavelength such as 632 nm, the n and k values increase in an increasing fashion. As the carbon concentration is linearly increased from 0 to some 41 atomic %, the index of refraction increases from 2.03 to 2.36 at 632 nm and the value of k increases from ~0.006 to ~0.304. Typical values of index of refraction for h-BN are 1.8 and 3.3 for B_4C.

4 Conclusions

Nanotechnology research requires the ability to fabricate and test many different material samples having defined, functionally graded, or static material properties or features at the 1 to 100 nm scale. PLD is a highly energetic and efficient technique to create thin film materials, but typically allows for only stoichiometric transfer of material from a single target material to substrate. As was demonstrated, using more than one physical target and programming a desired number of laser pulses onto each laser ablation target using a galvanometer resulted in a thin film material which had tailorable subnanometer mixing throughout the thin film from two exemplary pure target materials: BN and C. Typically, some 150 pulses at 300 mJ/pulse from the excimer laser resulted in 1 nm of material being deposited, demonstrating that island growth must occur on a per pulse basis. By calibration of the number of laser pulses per target to XPS or EDX composition ratios, any desired linear combination of B:C or other pure target materials can be achieved. By modeling the carbon content and the resulting index of refraction, a film containing a desired index of refraction (at 632 nm) between 2.02 and 2.36 could be deposited using this deposition technique. The amorphous nature and change of response with composition of each of the materials were verified using Raman spectroscopy. AFM can be used to measure the thickness, grain size, and RMS roughness of a sample, with typical roughness being shown to be on the order of 11 nm for samples which were not biased nor heated during deposition. Optical ellipsometry *in situ* was shown to be able to model the thickness of multiple layers, any combination of laser pulses, and all in real time while the laser is operating growing a film. Optical ellipsometry allows for all wavelengths from 370 to 1690 nm to be characterized simultaneously while depositing a thin film, and allows for the implementation of process control to be able to deposit thin films having specific thicknesses or optical properties, as is required for optical metamaterials, thermal materials, and nanotechnology applications.

Acknowledgments

References

1. T. Zehnder et al., "Determination of limits in deposition of adhering a-C films on silicon produced by pulsed laser deposition," *Thin Solid Films* **263**(2), 198–202 (1995), http://dx.doi.org/10.1016/0040-6090(95)06582-2.

2. A. Perrone et al., "Boron carbonitride films deposited by pulsed laser ablation," *Appl. Surf. Sci.* **133**(4), 239–242 (1998), http://dx.doi.org/10.1016/S0169-4332(98)00207-4.

3. K. Raidongia et al., "Synthesis, structure, and properties of homogeneous BC$_4$N nanotubes," *J. Mater. Chem.* **18**(1), 83–90 (2008), http://dx.doi.org/10.1039/b712472d.

4. D. Blank and H. Rogalla, "In-situ diagnostics at high pressures: ellipsometric and RHEED studies of the growth of YBa$_2$Cu$_3$O$_7$," *Mater. Res. Soc. Symp. Proc.* **502**, 237–247 (1997), http://dx.doi.org/10.1557/PROC-502-237.

5. G. E. Jellison, "Spectroscopic ellipsometry data analysis: measured versus calculated quantitites," *Thin Solid Films* **313–314**(1), 33–39 (1998), http://dx.doi.org/10.1016/S0040-6090(97)00765-7.

6. Md. Mannan et al., "Atomic arrangement, composition and orientation of hexagonal BCN films synthesized by radiofrequency plasma enhanced CVD," *J. Ceram. Soc. Jpn.* **117**(1364), 503–507 (2009), http://dx.doi.org/10.2109/jcersj2.117.503.

7. J. G. Jones, A. A. Voevodin, and J. S. Zabinski, "Characterization of plume fluence for laser ablation of yttria stabilized zirconia in mixed oxygen and argon environments," *Surf. Coat. Technol.* **146**(1), 258–262 (2001), http://dx.doi.org/10.1016/S0257-8972(01)01473-6.

8. A. Gorbunov et al., "Formation of unusual intermetallic phases by vacuum PLD," *Appl. Surf. Sci.* **197–198**(1), 475–480 (2002), http://dx.doi.org/10.1016/S0169-4332(02)00374-4.

9. G. E. Jellison and F. A. Modine, "Parameterization of the optical functions of amorphous materials in the interband region ," *Appl. Phys. Lett.* **69**(3), 371–373 (1996) [ibid 2137], http://dx.doi.org/10.1063/1.118064.

10. G. E. Jellison et al., "Characterization of pulsed-laser deposited amorphous diamond films by spectroscopic ellipsometry," *Mater. Res. Soc. Symp. Proc.* **526**, 349–354 (1998), http://dx.doi.org/10.1557/proc-526-349.

11. V. I. Merkulov et al., "Structure and optical properties of amorphous diamond films prepared by ArF laser ablation as a function of carbon ion kinetic energy ," *Appl. Phys. Lett.* **73**, 2591–2593 (1998), http://dx.doi.org/10.1063/1.122515.

12. S. Reich et al., "Resonant Raman scattering in cubic and hexagonal boron nitride," *Phys. Rev. B* **71**, 205201 (2005), http://dx.doi.org/10.1103/PhysRevB.71.205201.

13. A. Lousa, J. Esteve, and S. Muhi, "BCN thin films near the B4C composition deposited by radio frequency magnetron sputtering," *Diamond Relat. Mater.* **9**(3–6), 502–505 (2000), http://dx.doi.org/10.1016/S0925-9635(99)00319-2.

14. L. Song et al., "Large scale growth and characterization of atomic hexagonal boron nitride layers," *Nano Lett.* **10**(8), 3209–3215 (2010), http://dx.doi.org/10.1021/nl1022139.

15. E. Franke et al., "In situ infrared and visible-light ellipsometric investigations of boron nitride thin films at elevated temperatures," *J. Appl. Phys.* **84**(1), 526–532 (1998), http://dx.doi.org/10.1063/1.368083.

John G. Jones received the BS EE from Rose-Hulman Institute of Technology and the PhD from the University of Cincinnati. He is a senior materials research engineer for the USAF at the AFRL in the Materials and Manufacturing Directorate. Past research collaborations included process development of PLD processing of YBCO superconductors, HiPco for SWNT at Rice University, electronics for the MISSE-7 program, and thermal management materials. Current research focuses on PVD of thin films for nanoelectronics.

Lirong Sun received the PhD degree in the electro-optics graduate program from the University of Dayton, Ohio, in 2009. She is currently a senior scientist at General Dynamics Information Technology, working at the Air Force Research Laboratory. Her research interests are thin film coatings and characterizations of optical and structural properties of composited materials for optical thin film coatings and metamaterials applications.

Neil R. Murphy is currently a PhD student in materials engineering at the University of Dayton. He has been working within the Materials and Manufacturing Directorate at Wright Patterson Air Force Base since 2010, where his primary focus is on the deposition and characterization of optical thin films.

Tyson C. Back received the PhD in materials engineering from University of Dayton. He currently works for the Materials and Manufacturing Directorate at Wright-Patterson Air Force Base. His work at Wright-Patterson involves the characterization of carbon nanotube field emission cathodes. In addition to field emission measurements, surface analysis techniques are used to determine the surface chemistry and electronic structure of the cathodes before and after thin film deposition of low work function coatings.

Matthew A. Lange is a graduate of the Air Force Institute of Technology in applied physics. He has over 14 years' experience in experimental physics and mathematical modeling as applied to chemical kinetics, thin film deposition, material diagnostics, optical spectroscopy, plasma spectroscopy, electrodynamics, laser systems, directed energy effects, and plasma physics. He also authored or coauthored several journal articles, technical reports, and conference papers.

Jessica L. Remmert received the BS degree in physics-engineering from Washington and Lee University in 2005 and the MS degree in mechanical engineering from Georgia Institute of Technology in 2007. Her graduate level and subsequent research at the Air Force Research Laboratory's Materials and Manufacturing Directorate, Thermal Sciences Branch (WPAFB, Ohio) has emphasized the use of atomic force microscopy to characterize materials.

P. Terrence Murray received the PhD in physical chemistry from University of North Carolina (Chapel Hill) in 1979 and was a Welch Postdoctoral Fellow at the University of Houston until 1982, when he joined the University of Dayton (UD) Research Institute. He has over 25 years of experience in laser materials processing and holds a joint appointment as professor in the Graduate Materials Engineering program at UD.

Rachel Jakubiak is currently employed by the U.S. Air Force Research Laboratory (AFRL) where she investigates materials and optical properties of vacuum deposited thin films. While at AFRL her research areas have included random lasing, switchable polymer lasers, nonlinear optical measurements of third-order phenomenon, and multilayer coatings for optical band control. In 2012, she was elevated to senior membership status in SPIE and since 2007 has cochaired an SPIE conference on organic photonic materials.